# Supplementary Information for

# The Manipulation of Exchange Bias in van der Waal Ferromagnetic/Antiferromagnetic Heterojunction by Interfacial Coupling

*Guangcheng Wang[1], Lin Ma[2], Zijing Zhao[1], Shuaizhao Jin[3], Siyu Wang[2], Yao Yao[1], Meijiao Men[1], Pengying Chang[4], Yingzhou Yan[1], Yiyang Xie[4], Danmin Liu[2], Xueyun Wang[3], Xiaolei Wang[1,]**

[1]School of Physics and Optoelectronic Engineering, Beijing University of Technology, Beijing 100124, China

[2]Key Laboratory of Advanced Functional Materials, Ministry of Education, College of Materials Science and Engineering, Beijing University of Technology, Beijing 100124, China

[3]School of Aerospace Engineering, Beijing Institute of Technology, Beijing 100081, China

[4]Key Laboratory of Optoelectronics Technology of Ministry of Education, Beijing University of Technology, Beijing 100124, China

Corresponding authors:

Prof. *Xiaolei Wang*, Email: xiaoleiwang@bjut.edu.cn

## Crystal preparation

$Fe_3GaTe_2$ Crystal:

High-purity Fe power (99.99%), Ga lumps (99.99%) and Te power (99.999%) were mixed in an atomic ratio of 1:1:2 in quartz tubes under high vacuum, where Ga and Te also served as the flux. The quartz tubes are placed in a muffle furnace and heated to 1273 K in 1 h. After holding for 24 h, the temperature is rapidly lowered to 1153 K in 1 h. Then, the temperature is slowly lowered to 1053 K over a period of 120 h. Finally, single crystal of $Fe_3GaTe_2$ can be obtained by centrifugation.

$CrPS_4$ Crystal:

High-quality single crystals of $CrPS_4$ were synthesized by the chemical vapor transport method. Elements in the stoichiometric ratio of Cr:P:S = 1:1:4 were intimately mixed. The mixture was sealed in a vacuumed quartz tube, which was placed horizontally in a two-zone tube furnace. The temperature was set to 720 °C and 680 °C for the reaction and crystal growth region, respectively, for 8 days, followed by a furnace cooling to room temperature.

## Supplementary Figures

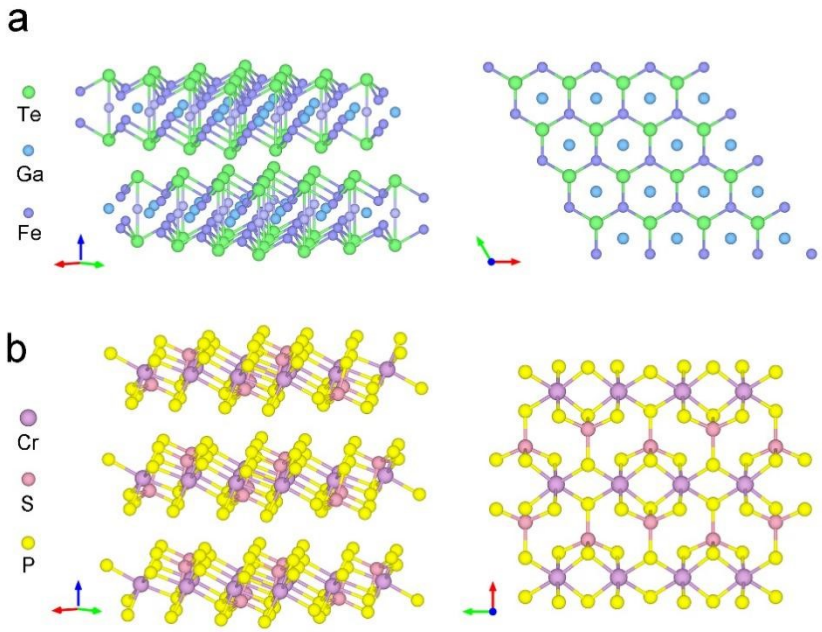


Fig. S1 Schematic diagram of the top view of the crystal structures, (a) $Fe_3GaTe_2$ (b) $CrPS_4$.

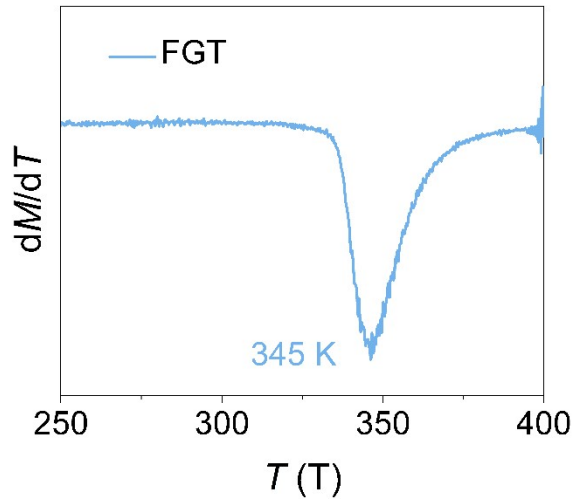


Fig. S2 The curve of the first derivative of magnetization with respect to temperature (d$M$/d$T$) for the $Fe_3GaTe_2$ nanoflake.

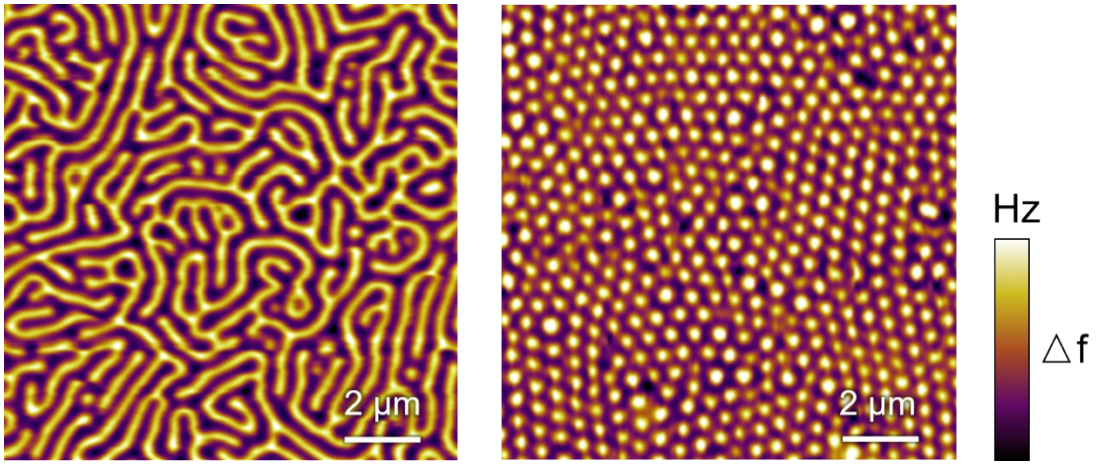


Fig. S3 Room-temperature labyrinthine domain (left) and skyrmion lattice (right) of the $Fe_3GaTe_2$ nanoflake.

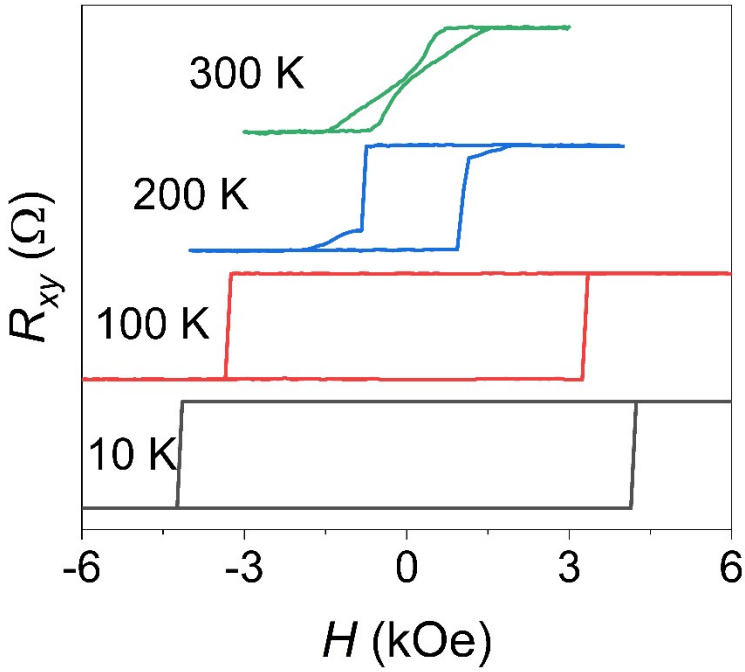


Fig. S4 Anomalous Hall effect hysteresis loops of a $Fe_3GaTe_2$ nanoflake at different temperatures.

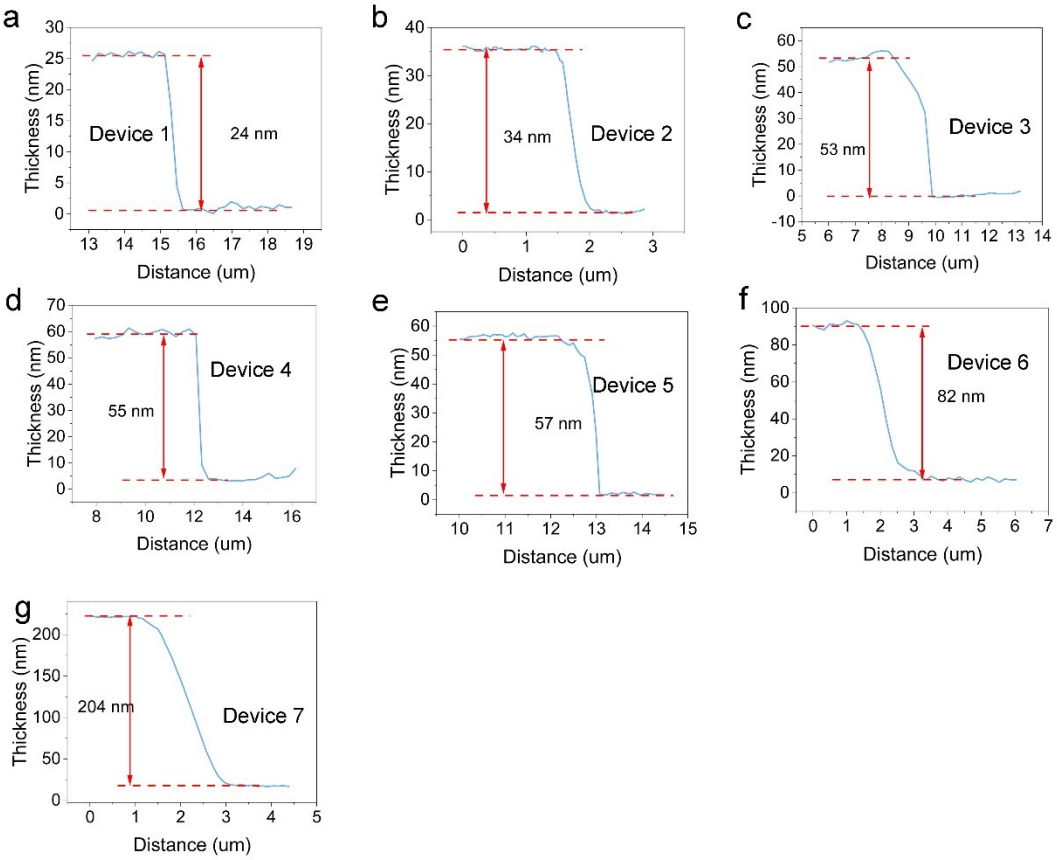


Fig S5. Different thicknesses of $Fe_3GaTe_2$ nanoflakes measured by atomic force microscope, which constitute the heterojunctions of (a) Device 1, (b) Device 2, (c) Device 3, (d) Device 4, (e) Device 5. (f) Device 6, and (g) Device 7.

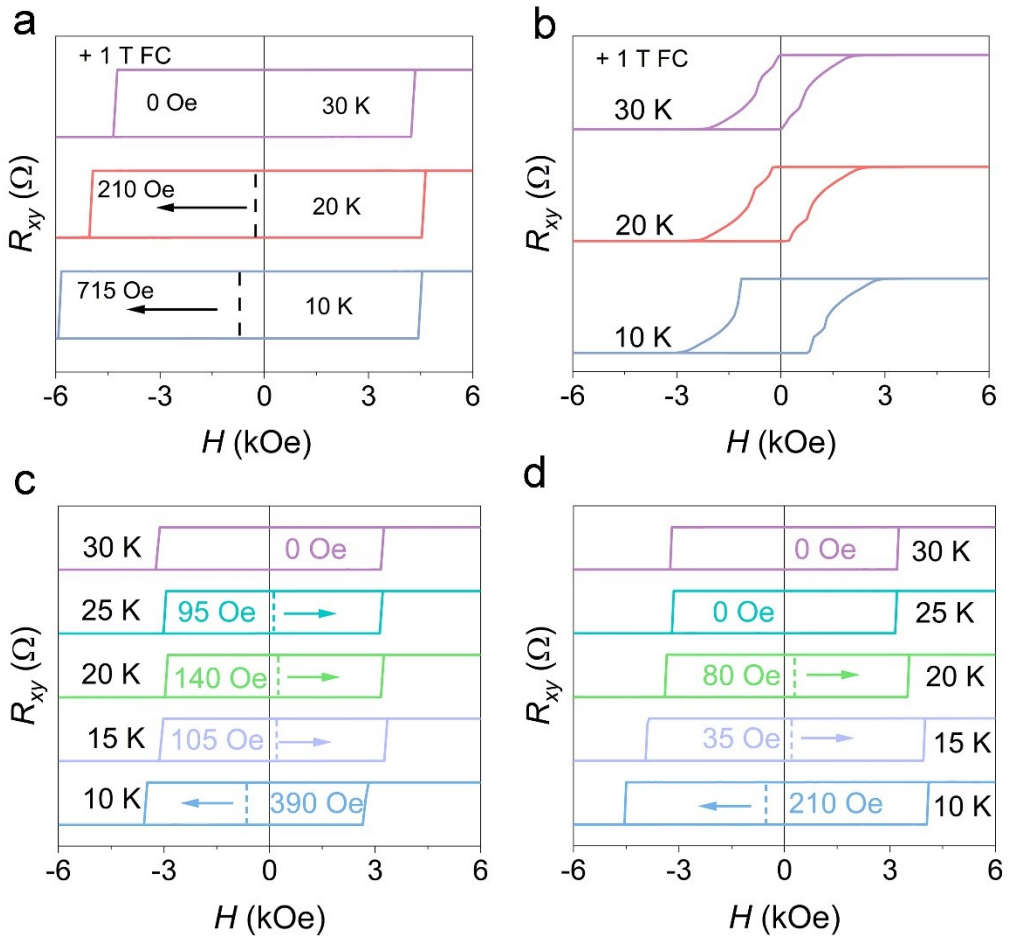


Fig S6 (a) $R_{xy}$-$H$ curves of Device 2 (34 nm) at 10 K, 20 K, and 30 K with a +1 T cooling field. (b) $R_{xy}$-$H$ curves of Device 7 (204 nm) at 10 K, 20 K, and 30 K with a +1 T cooling field. (c) $R_{xy}$-$H$ curves of Device 3 (53 nm) at 10 K-30 K with a +1 T cooling field. (d) $R_{xy}$-$H$ curves of Device 4 (55 nm) at 10 K-30 K with a +1 T cooling field.

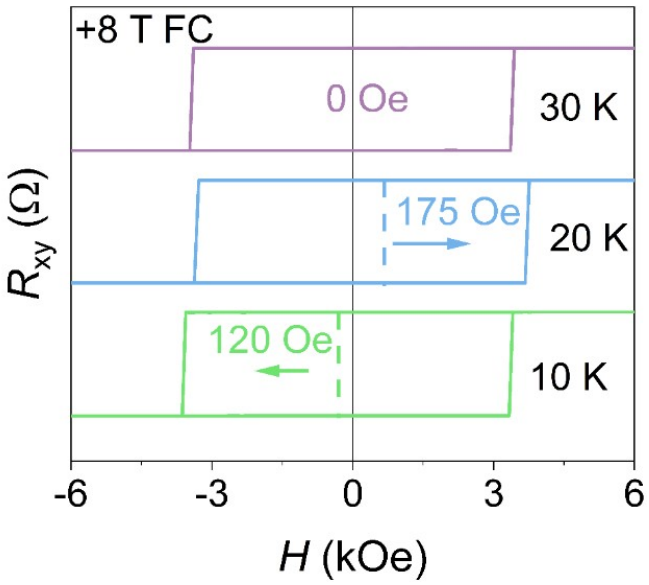


Fig S7. $R_{xy}$-$H$ curves of Device 5 at 10 K, 20 K, and 30 K with a +1T cooling field.

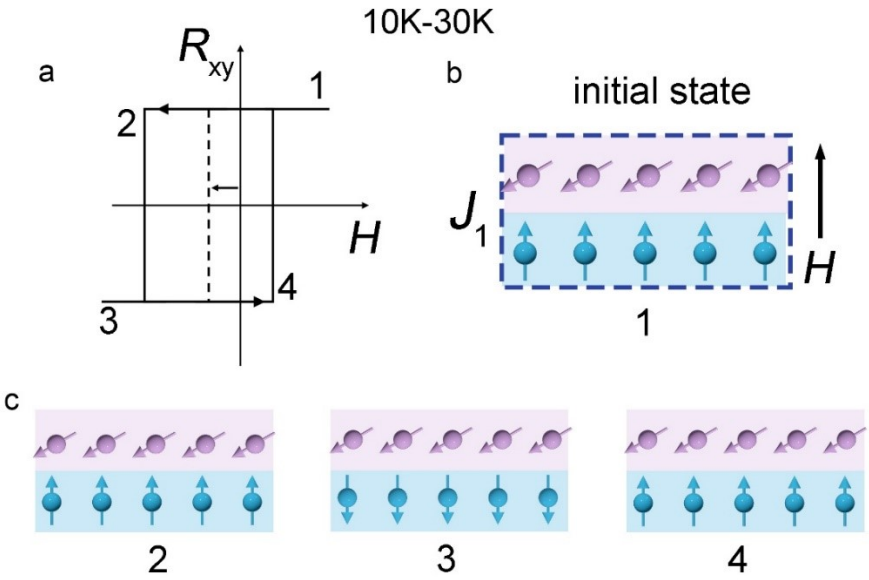


Fig. S8 The schematic model illustrating the origin of the negative exchange bias effect in thin Device at 10K-30K. (a) The schematic $R_{xy}$−$H$ curve of the thin Device with NEB. (b) The initial state before the magnetization reversal after field cooling. (b, c) Steps 1−4 reveal different magnetization reversal configurations marked in the $R_{xy}$−$H$ curve of (a).